Multi-section thermoelements, advantages and problems of their creation

© M.Yu. Shtern

National Research University of Electronic Technology,
124498 Moscow, Russia

E-mail: m.y.shtern@gmail.com

Received August 12, 2021
Revised August 28, 2021
Accepted August 28, 2021

In this work, the ways of increasing the efficiency of thermoelectric generators are considered. These include an increase in the figure of merit of thermoelectric materials, as well as an increase in the temperature difference between hot and cold junctions of thermoelements and, accordingly, the range of their operating temperatures. The expediency of using thermoelements with multi-section legs has been substantiated. For their creation, effective thermoelectric materials with operating temperatures in the range of 300−1200 K have been proposed. A technique for modeling such thermoelements has been developed. Structures and materials of effective contact systems for multi-section thermoelements have been proposed, a technology for their manufacture has been developed. Ways of switching sections in thermoelement legs are considered. The thermal expansion of thermoelectric materials is investigated and a method for damping thermal stresses in the design of a thermoelement is proposed. The problem of thermoelectric material sublimation at high temperatures was solved by using protective coatings.

Key words: thermoelectric generators, multi-section thermoelements, thermoelectric materials, thermal and electrophysical properties, contact systems, protecting coatings.

DOI: 10.21883/SC.2022.14.53847.02

1. Introduction

One of the main modern scientific directions is the creation of alternative energy sources and energy efficient technologies. Thermoelectricity could become one of these alternative technologies. Heat pumps operating on the Peltier effect are promising for converting low-potential energy of the earth and water sources for heating and air conditioning buildings [1–3]. Thermoelectric generators (TEG) are used wherever reliable power sources are required with a long service life and do not require maintenance. Huge opportunities lie in the use of TEG for the conversion of „waste“ heat, the share of which in the world energy production is more than 60% [4–6]. The efficiency of thermoelectric energy converters is mainly determined by the efficiency of semiconductor materials used for the manufacture of thermoelements. As a result of the intensive development of thermoelectricity in the middle of the 20th century, the efficiency of thermoelectric (TE) materials was achieved. The efficiency of TE materials is determined by their thermoelectric figure of merit (Z) or dimensionless parameter ZT, the value of which did not exceed 1.0. However, in order for thermoelectric devices to compete with traditional methods of cooling and power generation, it is necessary to increase the figure of merit of TE materials by a factor of 2−3. At the same time, there are no theoretical limitations for increasing ZT. In the last two decades, the activity of scientific research in the field of thermoelectricity has significantly increased. Effective TE materials were obtained with the ZT parameter equal to 1.2−1.4 [7–12]. These TE materials cover almost the entire operating temperature range for thermoelectric devices from 150 to 1300 K. At present, research is being actively carried out in order to obtain nanostructured TE materials. Thus, a decrease in the phonon component of thermal conductivity and, accordingly, an increase in ZT are achieved [6,7,13–16].

The widespread use of TEG is constrained by their low efficiency. The efficiency of modern TEG determined by formula (1) is 8% at best.

$$\eta = \frac{T_H - T_C}{T_H} \cdot \frac{\sqrt{(1 + Z\overline{T})} - 1}{\sqrt{(1 + Z\overline{T})} + T_C/T_H}, \qquad (1)$$

where T_H and T_C — temperature of hot and cold junctions of thermoelements, respectively; $\overline{T} = (T_H + T_C)/2$.

The efficiency of generators primarily depends on the figure of merit of the TE materials. In addition, the efficiency can be enhanced by increasing the temperature difference (ΔT) between the hot and cold junctions of the thermoelement and, accordingly, by expanding the operating temperature range of the TEG. For all TE materials, the figure of merit has a significant temperature dependence with the presence of a rather sharp maximum. Thus, the maximum values of the figure of merit of TE materials are available in a narrow (limited) temperature range. Therefore, to create effective TEG, it is necessary to use several different TE materials. It is possible to constructively realize this idea by means of the manufacture of multi-section thermoelements (MTE). Each section operates in a certain temperature range and is made of TE material, which has a maximum Z at these temperatures [8,17–23]. However, the creation of MTE is the most difficult structural and technological task that requires a number of problems to be solved. When designing the MTE, it is necessary

to optimize the dimensions of each section in the thermoelement legs. In addition to the electrical parameters of the thermoelement, the dimensions of the sections, namely, their height, determine the temperature range in which each section functions. One of the main tasks in the manufacture of efficient MTE is to ensure high-quality contact of the sections. To solve this problem, it is necessary to develop the technology of contact systems (CS), consisting of contact layers. These layers perform the following functions: carry out ohmic contact with the TE material; are a diffusion barrier that prevents the interdiffusion of the materials to be joined; provide the necessary adhesion of the contact layers to the TE material. It should be noted that the latter function is important, since this adhesion is a limiting factor in the mechanical strength of the thermoelement. In the MTE technology, it is necessary to obtain thermostable contacts with an adhesive strength of at least 8 MPa and a contact resistance not exceeding $10^{-8}\,\Omega \cdot m^2$ [2,15,17,23–29]. There are several methods for forming a CS. Prospective is their production by vacuum deposition [19,23,27,30], which provides a minimum value of contact resistance and high adhesion. In the design of MTE, several TE materials with different values of the thermal coefficient of linear expansion (T*CLE) are used. This complicates the situation, since significant mechanical stresses arise in the thermoelement, which can lead to its destruction. In this regard, it seems expedient to create a CS structure, which, while performing its main functions, additionally is a damper layer. Another problem in the design of high-temperature MTE, which has been studied to a limited extent [31,32], is the sublimation of TE materials at high temperatures. For such temperatures, it is necessary to develop and research protective coatings.

In connection with the above, the purpose of this work is to determine ways to solve the problems associated with the creation of multisection thermoelements for TEG with operating temperatures up to 1200 K.

2. Researtch methods

To determine the elemental composition of the obtained TE materials and contact layers, a JEOL JSM 6480LV scanning electron microscope with an INCA ENERGY Dry Cool attachment for energy-dispersive X-ray spectrometry was used. The limit of the relative error of the measurement method does not exceed 5%.

The study of thermoelectric parameters of TE materials was carried out using the developed technique and measuring complex presented in [33]. The technique allows to carry out studies of electrical conductivity, Seebeck coefficient and thermal conductivity of materials in the range of 300−1200 K. Measurement errors are: electrical conductivity and Seebeck coefficient — 3%; thermal conductivity — 5%.

The roughness of the surface of the samples intended for deposition contacts after mechanical treatment was determined using a KLA-Tencor P-7 profilometer. The same device was used to measure the thickness of the deposited Ni layers with an error not exceeding 5%.

The measurement of the adhesion strength of the CS formed on the TE materials was carried out by the method of uniform normal tear on the Force Gauge PCE-FM50 installation. For this purpose, contacts with an area of $1\,mm^2$ were formed using photolithography. The adhesion strength was measured in terms of the tear force per unit area (Pa). The measurement error did not exceed 5%.

The contact resistance of the CS was determined using a technique developed by the authors. It is based on the measurement of the total electrical resistance, consisting of the transient contact resistance and the resistance of the TE material, with its subsequent exclusion.

To determine the thermal stability of the CS, the samples were annealed in vacuum at their operating temperatures for 60 min. After thermal treatment, the CS was studied by Auger electron spectroscopy (AES) on a raster Auger-electronic spectrometer PHI-670xi with a field emission Schottky thermocathode.

The thermal stability of TE materials was assessed using differential scanning calorimetry on a Shimadzu DSC-50 calorimeter. 5 measurements of each sample were carried out in a nitrogen atmosphere (20 ml/min) at a heating rate of 10 degrees per minute.

Thermogravimetric analysis for the study of sublimation evaporation of TE materials was carried out using a TA Instruments SDT Q600 thermal analyzer. The sensitivity of the device for determining the change in mass is $0.1\,\mu g$. The heating rate of the samples was 10 K per minute. The measurements were carried out on 5 samples of each TE material.

To study the TCLE, we used a dilatometric method based on quartz dilatometers. To determine the TCLE of low-temperature TE materials, a technique based on a thermoelectric thermostat was used [34]. The TCLE studies were also carried out on a high-precision horizontal dilatometer L75 PT with an operating temperature range from 300 to 1700 K.

3. Experimental part and discussion

3.1. Thermoelectric materials

For MTEs with operating temperatures from 300 to 1200 K, effective TE materials have been obtained. Using energy-dispersive X-ray spectrometry, the chemical composition of the obtained TE materials was determined. Studies of temperature dependences of thermoelectric parameters of TE materials have been carried out. The data obtained were used to calculate Z and the dimensionless parameter ZT, the temperature dependences of which are shown in Fig. 1. The results of the temperature dependence of ZT make it possible to determine the ranges of operating temperatures of TE materials, where they have the maximum values of ZT.

For temperatures up to 400 K, *n*-type conductivity $Bi_2Te_{2.8}Se_{0.2}$ (0.14 wt% $CdCl_2$) and *p*-type conductivity $Bi_{0.5}Sb_{1.5}Te_3$ (2 wt% Te, 0.14 wt% TeI_4) with maximum ZT equal to 1.05 and 1.11 respectively, were prepared by zone melting.

For the temperature range 400−600 K, $Bi_2Te_{2.4}Se_{0.6}$ (0.18 wt% CuBr) *n*-type and $Bi_{0.4}Sb_{1.6}Te_3$ (0.12 wt% $PbCl_2$, 1.50 wt% Te) *p*-type were obtained by extrusion with maximum ZT equal to 1.19 and 1.20, respectively. In the temperature range 600−900 K, the maximum ZT values of 1.08 and 1.20 are found for *n*-type PbTe (0.2 wt% PbI_2, 0.3 wt% Ni) and *p*-type GeTe (7.4 wt% Bi) respectively. These materials are obtained by hot pressing. For operating temperatures of 900−1200 K by the method of spark plasma sintering, *n*- and *p*-type materials were obtained: $Si_{0.8}Ge_{0.2}$ (2.2 wt% P) and $Si_{0.8}Ge_{0.2}$ (1.8 wt% B), with maximum ZT equal to 1.04 and 1.03, respectively.

3.2. Modeling multisection thermoelement

As indicated above, the maximum efficiency of MTE will be if each section and, accordingly, the TE material from which it is made operate in the temperature range where ZT has high values (Fig. 1). For this, it is necessary to optimize the design of the MTE. For this purpose, a methodology for modeling MTE and software for its implementation has been developed. When modeling the MTE design, the main data are the thermal and electrophysical parameters of the TE materials and their temperature dependences. Simulation boundary conditions: temperatures of hot (T_H) and cold (T_C) junctions and temperature difference ($\Delta T = T_H - T_C$) as well as the maximum permissible height of the thermoelement. As a result of modeling, the optimal height of the sections in the legs of the MTE is determined, at which the TE materials has the maximum ZT. As a result, it allows to obtain the maximum values of efficiency for MTE. Optimization of the MTE design is carried out as follows. The height of each section (l_{ni}, l_{pj}), depends on the operating temperature range of the sections ($T_{ni} - T_{ni-1}$, $T_{pj} - T_{pj-1}$) and the thermal conductivity coefficients of the TE materials (κ_{ni}, κ_{pj}), where i, j are the section numbers for the *n*- and *p*-types. First, according to the experimental data, the average values of the Seebeck coefficient ($\overline{s}$), electrical conductivity ($\overline{\sigma}$) and thermal conductivity ($\overline{\kappa}$) coefficients are calculated for each section in the operating temperature range. Next, the height of each section is determined. The calculation is based on the fact that the heat flux passing from the hot junction to the cold one through each section has a constant value:

$$\frac{\overline{\kappa}_{n1}\Delta T_{n1}}{l_{n1}} = \frac{\overline{\kappa}_{ni}\Delta T_{ni}}{l_{ni}} = \ldots = \frac{\overline{\kappa}_{nN}\Delta T_{nN}}{l_{nN}};$$
$$\frac{\overline{\kappa}_{p1}\Delta T_{p1}}{l_{p1}} = \frac{\overline{\kappa}_{pj}\Delta T_{pj}}{l_{pj}} = \ldots = \frac{\overline{\kappa}_{pP}\Delta T_{nP}}{l_{pP}}, \qquad (2)$$

where ΔT_{ni} and ΔT_{pj} — temperature difference on i and j sections of *n*- and *p*-legs; N and P — number of sections

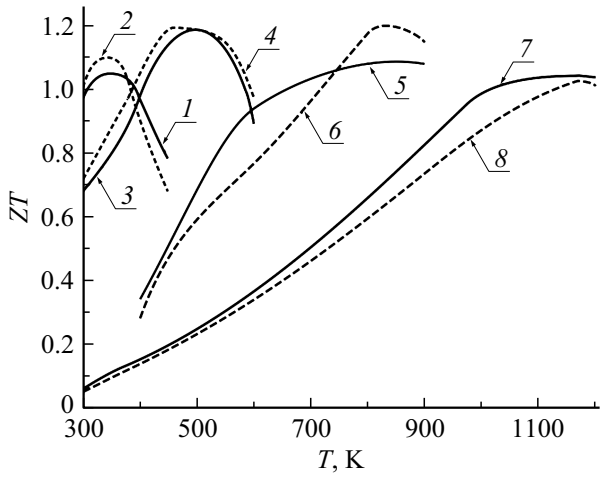

Figure 1. Temperature dependences of the parameter ZT of TE materials. *1* — $Bi_2Te_{2.8}Se_{0.2}$, *2* — $Bi_{0.5}Sb_{1.5}Te_3$, *3* — $Bi_2Te_{2.4}Se_{0.6}$, *4* — $Bi_{0.4}Sb_{1.6}Te_3$, *5* — PbTe, *6* — GeTe, *7* — $Si_{0.8}Ge_{0.2}$ (*n*-type), *8* — $Si_{0.8}Ge_{0.2}$ (*p*-type).

of *n*- and *p*-legs; $\overline{\kappa}_{ni}$ and $\overline{\kappa}_{pj}$ — the averaged value of the thermal conductivity coefficient in the range of working temperatures of i and j sections.

The sums of the heights of the sections of the *n*- and *p*-legs must be equal between themselves and correspond to the given size of the MTE legs. The same applies to the temperature difference between the hot and cold junctions of the MTE:

$$L_{n,p} = \sum_{i=1}^{N} l_i = \sum_{j=1}^{P} l_j; \quad \Delta T = \sum_{i=1}^{N} \Delta T_{ni} = \sum_{j=1}^{P} \Delta T_{pj}. \quad (3)$$

The temperature profile of the MTE legs is determined by $\overline{\kappa}_{nj}$ and $\overline{\kappa}_{pj}$. Thermal conductivity data were obtained as a result of studies of TE materials. In addition, the temperature ranges are known in which the maximum values of ZT are observed (Fig. 1). In this regard, from equations (3), you can calculate the height of the i-th or j-th sections as follows:

$$l_{ni} = \frac{L_{p,n}\overline{\kappa}_{ni}\Delta T_{ni}}{\overline{\kappa}_n \Delta T}; \; l_{pj} = \frac{L_{p,n}\overline{\kappa}_{pj}\Delta T_{pj}}{\overline{\kappa}_p \Delta T}. \qquad (4)$$

As a result of modeling the MTE using the boundary conditions ($T_H = 1200$ K; $T_C = 300$ K; the maximum height of the MTE legs is 20 mm), the MTE design is shown in Fig. 2.

The developed technique is focused on obtaining the maximum efficiency. For the MTE shown in Fig. 2, the efficiency, excluding heat and electrical losses at the contacts, is 21.5%. This is consistent with the data [17,35]. The calculated efficiency value for a thermoelement made of TE materials based on $Si_{0.8}Ge_{0.2}$, at $\Delta T = 900$ K, without taking into account losses, is 12%. This confirms the feasibility of designing MTEs.

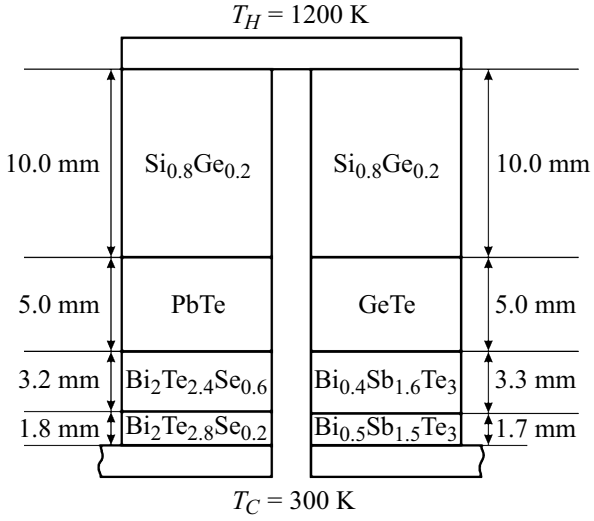

Figure 2. The design of the multi-section thermoelement.

3.3. Contact systems

Obtaining high-quality contact systems is the main problem in the development of MTEs. To form the contact layers in the CS, we used the methods of vacuum deposition in conjunction with the chemical deposition of the connecting layers. The state of the surface of TE materials, on which the CSs are formed, is a decisive factor for their adhesion, and also has a significant effect on the contact resistance. Before the formation of the CS, the surface of TE materials was subjected to mechanical treatment according to the technique [19]. It is important to obtain a given surface roughness, which significantly affects the adhesion of the film. With a roughness commensurate with the thickness of the film, its discontinuity formation are possible and, as a consequence, a decrease in adhesion and an increase in the electrical resistance of the contacts [23]. Films with a thickness of 300 nm and higher were used as the first layers of the CS. Therefore, the surface of TE materials was processed with a roughness not exceeding 200 nm. Before loading into the chamber of the sputtering system, the samples were washed in isopropyl alcohol, followed by drying in a nitrogen flow. Vacuum-thermal annealing of the samples was carried out directly in the chamber at an initial pressure of $7 \cdot 10^{-8}$ Torr and the temperature of 473 K. After annealing, the surface of the samples was cleaned by bombardment with argon ions for 30 seconds.

Contacts can be made of one material, for example, Ni or Co, which is possible at low temperatures [23,27]. However, at elevated temperatures, which are typical for MTEs, it is necessary to use CSs consisting of several contact layers. In this case, each layer in the CS structure performs its own functions, which were mentioned above. The first layer in the CS structure, which is formed directly on the TE material, should provide ohmic contact with the TE material. This layer mainly determines the adhesive strength of the contact. A necessary condition for the existence of an ohmic contact at the metal–semiconductor interface is a low value of the Schottky barrier. The Schottky barrier is determined by two mechanisms of conduction: thermionic emission and tunneling [36]. For most semiconductors, it was experimentally found that the energy barrier does not depend on the work function of the metal, but is determined by the density of surface states [36–38]. In this regard, a method for making ohmic contacts is widely used-heavy doping of a semiconductor at the contact. The dominant tunneling current component exponentially depends on the concentration of free current carriers [37]. At a concentration of about 10^{19} cm^{-3} the contact resistance is determined mainly by tunneling processes. It should be noted this positive effect for TE materials with a carrier concentration, as a rule, exceeding 10^{19} cm^{-3}.

To ensure ohmic contact, it is necessary to use materials of contact layers with low resistivity, for example: Mo, W, Co and Ni [23]. For low temperatures, Ni obtained by vacuum deposition has proven itself well [19,27,28,39]. The AES studies of samples with Ni contacts 400−500 nm thick after thermal treatment in vacuum at 577 K showed that at this temperature Ni ceases to function as a barrier layer [23,27]. Thus, it is advisable to use nickel contacts at temperatures up to 500 K. Above this temperature, Ni can be used in combination, for example, with Mo [23,27].

For thermoelements operating at elevated temperatures, it is necessary to use a diffusion-barrier layer (DBL) in the CS structure. In work [23], on the basis of the physicochemical analysis of the reasons for the stability and degradation of the DBL, we substantiated the criteria and determined the DBL materials that provide high temperature stability of the CS. The most promising for DBL are materials such as Mo, Nb, Ta, W. At high temperatures, it is advisable to use amorphous materials as DBL [23]. Films of the Ta-W-N alloy formed by the method of magnetron sputtering were used as an amorphous layer in the CS. Thus, according to the criteria defined above, the following structures and materials of the CS layers were selected. Nickel films up to 400 nm thick were used at temperatures up to 500 K. Above this temperature, a two-layer Mo/Ni CS was used. The Mo layer 300−400 nm thick provided a low-resistance contact and adhesion of the CS to TE materials, and also served as a DBL. The Ni layer, up to 400 nm thick, was used as a commutation layer. At high temperatures, it is advisable to use CS Mo/Ta-W-N/Ni. The Ta-W-N layer 400 nm thick, in addition to the barrier functions of Mo, significantly enhanced the DBL.

The deposition of the contact layers of the CS was carried out in a single vacuum cycle on an URM 3.279.026 ion-plasma sputtering unit equipped with two magnetron systems. The formation of a Ni-based CS was carried out by sputtering a Ni target. The Mo/Ni CS was deposited by sequential sputtering, first target Mo, then Ni. The formation of a three-layer Mo/Ta-W-N/Ni CS was carried out by sequential sputtering, first of a Mo target in an argon atmosphere, and then a Ta-W composite target in a mixture of argon and nitrogen gases.

Table 1. Samples of TE materials and structures of the CS formed on them

№	Samples of TE materials	Structures of CS
1	$Bi_2Te_{2.8}Se_{0.2}$	Ni (400 nm)
2	$Bi_{0.5}Sb_{1.5}Te_3$	Ni (400 nm)
3	$Bi_{0.4}Sb_{1.6}Te_3$	Mo (300 nm)/Ni (400 nm)
4	$Bi_2Te_{2.4}Se_{0.6}$	Mo (300 nm)/Ni (400 nm)
5	PbTe (600 K) PbTe (850 K)	Mo (400 nm)/Ni (400 nm) Mo (400 nm)/Ta-W-N (400 nm)/Ni (400 nm)
6	GeTe (600 K) GeTe (850 K)	Mo (400 nm)/Ni (400 nm) Mo (400 nm)/Ta-W-N (400 nm)/Ni (400 nm)
7	$Si_{0.8}Ge_{0.2}$ (P)	Mo (400 nm)/Ta-W-N (400 nm)/Ni (400 nm)
8	$Si_{0.8}Ge_{0.2}$ (B)	Mo (400 nm)/Ta-W-N (400 nm)/Ni (400 nm)

Table 2. Adhesion strength and resistivity of CS

TEM samples	Adhesive strength of CSs, MPa	Contact resistivity $\Omega \cdot m^2$
$Bi_2Te_{2.8}Se_{0.2}$	15.72	$0.8 \cdot 10^{-9}$
$Bi_{0.5}Sb_{1.5}Te_3$	15.64	$0.9 \cdot 10^{-9}$
$Bi_{0.4}Sb_{1.6}Te_3$	14.56	$0.9 \cdot 10^{-9}$
$Bi_2Te_{2.4}Se_{0.6}$	14.42	$1.0 \cdot 10^{-9}$
PbTe (600 K)	14.12	$1.1 \cdot 10^{-9}$
PbTe (850 K)	14.08	$1.3 \cdot 10^{-9}$
GeTe (600 K)	14.24	$1.1 \cdot 10^{-9}$
GeTe (850 K)	14.20	$1.4 \cdot 10^{-9}$
$Si_{0.8}Ge_{0.2}$ (P)	14.73	$1.5 \cdot 10^{-9}$
$Si_{0.8}Ge_{0.2}$ (B)	14.64	$1.5 \cdot 10^{-9}$

Each leg of the MTE consists of four sections made of different TE materials (Fig. 2). On TE materials, taking into account their operating temperatures, the CSs were formed, presented in Table 1.

Measurements of adhesion strength and specific contact resistance of CS formed on TE materials, indicated in Table 1. On all samples, the contact was destroyed along the TE material-CS interface. The measurement results are presented in Table 2.

On TE materials operating at temperatures up to 400 K (Fig. 2), single-layer nickel CSs with a thickness of 400 nm were formed. The obtained CSs had good adhesion strength exceeding 15 MPa and low specific contact resistance, of the order of $10^{-9}\ \Omega \cdot m^2$. On TE materials operating at temperatures up to 600 K, Mo with a thickness of 300–400 nm was used as a barrier layer. The Ni commutation layer was deposited 400 nm thick. Such CSs were formed on $Bi_{0.4}Sb_{1.6}Te_3$ and $Bi_2Te_{2.4}Se_{0.6}$ samples, as well as on PbTe and GeTe samples, at their operating temperatures up to 850 K. The adhesion strength of the obtained CS decreased slightly (by 6–7%). Change in the contact resistance of the CS within the measurement error. For temperatures of 850 K and higher, DBL was enhanced on PbTe and GeTe samples and samples based on $Si_{0.8}Ge_{0.2}$ by introducing an amorphous Ta-W-N layer 400 nm thick into the CS. For the obtained CSs, the adhesive strength remained practically unchanged. In this case, there is a slight increase in the contact resistance due to the amorphous layer (Table 2).

To study the thermal stability of the CS, the samples were annealed in vacuum at the operating temperatures of each TE material for 60 min. After that, using Auger electron spectroscopy, a study of AES was carried out — the profile of the distribution of elements over the depth of the CS. In this case, layer-by-layer ion sputtering of the surface of the samples was used. As an example of the research results, AES are given — profiles of the distribution of elements over a depth of about 900 nm from the surface of GeTe and PbTe samples (Fig. 3).

To study the thermal stability of CS-Mo (400 nm)/Ni (400 nm), the samples were annealed in vacuum at 800 K for 60 min. The figure clearly shows pronounced Ni layers with a thickness of about 400 nm and layers of Mo (400 nm) deposited directly on the TE material. It is important to note the absence of penetration of elements of TE materials through DBL from Mo. Thus, it can be concluded that CSs are thermally stable at temperatures up to 800 K.

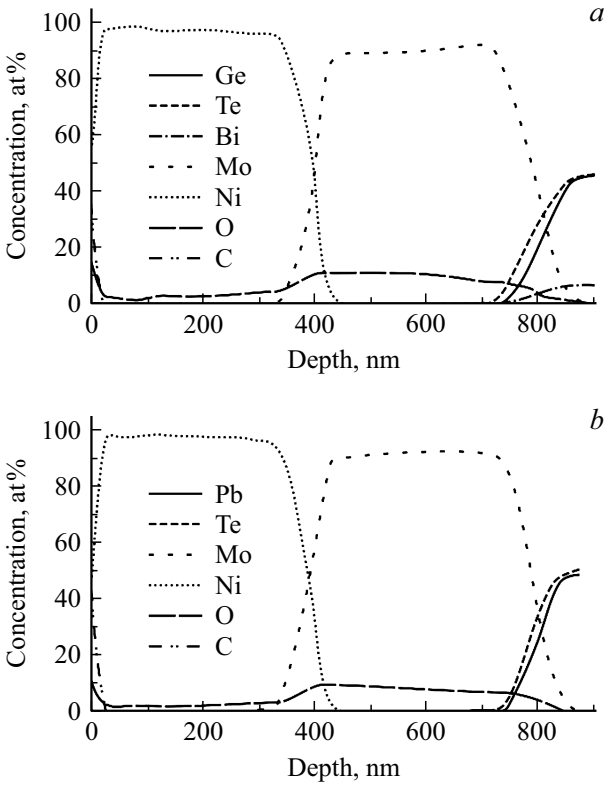

Figure 3. AES — profiles of the distribution of elements over the depth of the samples: (*a*) GeTe + Mo (400 nm) + Ni (400 nm); (*b*) PbTe + Mo (400 nm) + Ni (400 nm).

Also, studies of AES were carried out — the profiles of the distribution of elements in depth on other TE materials with CS, presented in Table 1. The results of the study showed the thermal stability of the CS.

3.4. Commutation of thermoelement

For commutation sections in MTE, an increased thickness of the commutation layer is required. For this purpose, we used the chemical deposition of Ni on the above CS. Deposition was carried out from a borohydride electrolyte at temperatures of 360 K for 60 min. The thickness of the deposited films was $17-20\,\mu$m. Using energy-dispersive X-ray spectrometry, the chemical composition of the obtained films was determined, in which Ni was found to be 96.84 wt%. The main other elements are: C — 1.85 wt%; O — 1.17 wt%.

The sections were commutated in the MTE structure in several ways. Commutation of low-temperature sections in the legs of the MTE was carried out using soldering. At elevated temperatures, in addition to high-temperature soldering, the methods used for commutation were realized by means of: the formation of a Ni-In alloy; Ni-Sn eutectic alloy; using bonding of Au-Au layers.

The sections were commutated using the Ni-In intermetallic compound as follows. On the surfaces to be joined on a Ni layer, a galvanic In layer $2\,\mu$m thick was formed in the galvanostatic mode in an electrolyte based on $In_2(SO_4)_3$ and Na_2SO_4 at a temperature of 300 K. The splicing of the sections was carried out under pressure at 570 K, followed by an increase in temperature to 670 K for 30 min. To commutate the sections using a Ni-Sn eutectic alloy, a 2-μm-thick tin layer was formed on the CS nickel layer by vacuum thermal evaporation on a UVN71R-1 installation. The splicing of the sections was carried out under pressure in a box with an inert atmosphere at a temperature of 600 K for 30 min.

Bonding is a promising method of commutation sections, which ensures the splicing of the Au-Au commutation layers. To perform bonding operations, V (50 nm) and Au (500 nm) layers were formed on the surface of the Ni commutation layer in the CS. The deposition of these layers was carried out on a Kurt J. Lesker Company electronic deposition system of metals at a pressure in a vacuum chamber no higher than $7.5 \cdot 10^{-7}$ Pa and an accelerating voltage of 10^4-10^5 W/cm. The bonding operation was carried out on a SUSS MicroTec FC150 FLIP CHIP BONDER device at the following modes: temperature 610 K; pressing force of the connected sections up to 850 N, time 25 min. To determine the quality of the joints of sections in MTE based on lead and germanium tellurides with sections based on SiGe, the method of uniform normal tear was used. Separation of the joints occurred at loads exceeding 14 MPa along the TE material-CS boundary. That is, the mechanical strength of the joint of the sections was determined by the adhesion strength of the CS. The bonded commutation was not disturbed.

3.5. Thermal expansion of materials

Using quartz dilatometers of various designs, the thermal expansion of the developed TE materials in the temperature range of 200–1200 K was studied. The average value of the TCLE was determined by the formula [40]:

$$\overline{\alpha} = (L_T - L_0)/\big(L_0 \cdot (T - T_0)\big), \qquad (5)$$

where L_T is the sample length at the final temperature, L_0 is the sample length at T_0.

The mean TCLE calculated in this way refers to the final temperature of the interval (T). The results of the study of the TCLE of TE materials of n- and p-type conductivities are presented in Fig. 4. As a result of the study of low-temperature TE materials in the range of 200–400 K, the average TCLE of $Bi_2Te_{2.8}Se_{0.2}$ varies from $14.5 \cdot 10^{-6}\,K^{-1}$ to $14.8 \cdot 10^{-6}\,K^{-1}$, and $Bi_{0.5}Sb_{1.5}Te_3$ from $13.9 \cdot 10^{-6}\,K^{-1}$ to $15.0 \cdot 10^{-6}\,K^{-1}$. Thus, the TCLEs of these materials have similar values. For medium-temperature TE materials: $Bi_2Te_{2.4}Se_{0.6}$ and $Bi_{0.4}Sb_{1.6}Te_3$, the studies were carried out in the temperature range from 300 to 600 K. The TCLE of the materials under consideration after 350 K has an almost constant value at the level of $(13.93-14.33) \cdot 10^{-6}\,K^{-1}$. lose values of TCLE for bismuth and antimony tellurides were obtained in [25].

The TCLE values of PbTe in the range 600–900 K vary from $20.14 \cdot 10^{-6}\,K^{-1}$ to $23.07 \cdot 10^{-6}\,K^{-1}$ at 900 K. Similar values of TCLE were obtained in [41,42]. For GeTe, a sharp increase in TCLE in the temperature range of 620–680 K is associated with a change in the structure at these temperatures from the rhombohedral to cubic type of NaCl, which is described in [43,44]. Subsequently, as the temperature rises, the TCLE increases, reaching $24.47 \cdot 10^{-6}\,K^{-1}$ at 900 K. At the maximum operating temperatures, the TCLEs of PbTe and GeTe do not differ significantly. The presented results agree with the X-ray data obtained by other authors: PbTe [41] and GeTe [43].

The thermal expansion of high-temperature TE materials based on SiGe has been studied extremely limitedly by the dilatometric method [45] and on the basis of X-ray data [46]. As expected, the temperature dependences of the TCLE of n- and p-type SiGe practically do not differ (Fig. 4). With an increase in temperature, TCLE decreases from $7 \cdot 10^{-6}\,K^{-1}$ (300 K) to $4.5 \cdot 10^{-6}\,K^{-1}$ at 500 K. Further, with temperature, the TCLE increases insignificantly, reaching a maximum value of $4.8 \cdot 10^{-6}\,K^{-1}$ at 1180 K. Above this temperature, there is an anomaly associated with a tendency towards a decrease in TCLE. The obtained results on the TCLE are in agreement with the data for pure silicon [47].

Analyzing the results of the TCLE study, it should be noted that the TCLE of materials based on PbTe and GeTe differs significantly from the TCLE of SiGe. In the temperature range of 900 K, at which the sections made of these materials are in contact, the TCLE differ by a factor of 6. This requires the adoption of structural solutions that provide damping of mechanical stresses arising in the

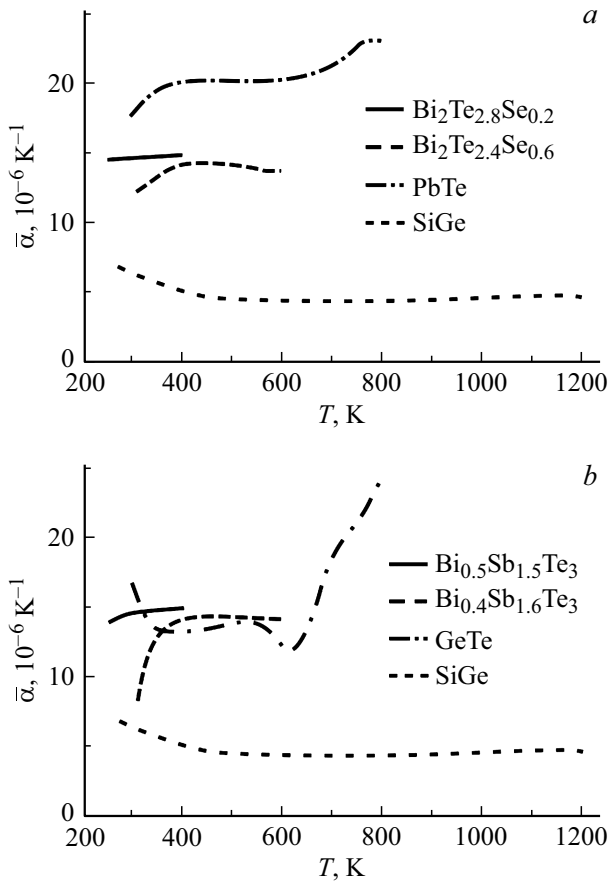

Figure 4. Temperature dependences of TCLE for *n*-type (*a*) and *p*-type (*b*) TE materials.

process of thermal cycling of MTE. For this purpose, we propose to form a layer of composite material in the CS structure in sections that differ significantly in TCLE in the following way. An array of carbon nanotubes is grown on the formed CS structure by chemical vapor deposition at a temperature of 820 K for 5 min. After that, by the method of chemical deposition, metallic nickel, which is a conductive material, is deposited from a solution of a nickel salt. Ni fills the space between carbon nanotubes. At the final stage, the structure is heat treated in vacuum at a temperature of 920 K for 60 min. As a result, nickel wets carbon nanotubes and flows between them, forming a composite conducting material. The CS obtained in this way increases the mechanical strength and increases the thermal resistance of the thermoelement [48].

3.6. Thermal stability of materials

The evaluation of the thermal stability of the investigated TE materials during thermal cycling was carried out using the methods of differential scanning calorimetry and thermogravimetry. Researches of $Bi_2Te_{2.8}Se_{0.2}$; $Bi_{0.5}Sb_{1.5}Te_3$; $Bi_2Te_{2.4}Se_{0.6}$; $Bi_{0.4}Sb_{1.6}Te_3$ were carried out in the temperature range 300–600 K. On the obtained DSC curves, no thermal effects were observed with an increase in temperature from 300 to 600 K due to phase transitions. The results were obtained for all the indicated TE materials, regardless of the composition and methods of their preparation. Thermogravimetry was used to estimate the change in the mass of TE materials. Studies have shown that an increase in temperature does not lead to a significant change in the mass of samples for all TE materials at temperatures of 300–600 K. The absence of a noticeable change in weight during thermal cycling indicates that sublimation and oxidation of TE materials are not observed in the investigated temperature range. The thermal stability of TE materials based on PbTe and GeTe was investigated in the temperature range 300–900 K and TE materials based on *n*- and *p*-type SiGe in the range 300–1200 K. On the obtained DSC curves, no obvious thermal effects were observed over the entire temperature range of measurements. Thus, it can be noted that the materials under study are thermally stable in the indicated temperature ranges for each TE material. In the study using thermogravimetry of sublimation and oxidation in the working temperature ranges, the following was observed. For TE materials based on SiGe, the mass of the samples decreases insignificantly up to a temperature of 1200 K. Above 850 K, a sharp decrease in the mass of the samples begins for PbTe and GeTe, which indicates the onset of sublimation of these materials. The research results show that when choosing the range of operating temperatures of TE materials, it is necessary to take into account not only the temperature dependences of their thermoelectric parameters, but also the thermal stability of materials. For example, for PbTe and GeTe, the upper operating temperature range should be limited to 850 K.

To exclude negative oxidation and sublimation processes, it is advisable to use protective coatings for thermoelements. With the help of this technique, it is possible to increase the range of operating temperatures. The layers of Si_3N_4 and SiO_2 were studied as protective coatings. The deposition of these layers was carried out by the plasma-chemical method (CORIAL D250 setup); the layer thicknesses were 1.0 and 0.25 μm, respectively. The formation of protective coatings was carried out at a temperature of 520 K. Thermogravimetric studies have shown the effectiveness of these protective coatings up to a temperature of 1200 K.

4. Conclusion

Effective TE materials have been developed for the operating temperature range of 200–1200 K with a figure of merit *ZT* from 1.03 to 1.20, which are used for fabricating MTE sections. A method, mathematical models, and software for modeling MTE have been developed. As a result, the design of the MTE was optimized and the value of its efficiency was calculated. Excluding heat and electrical losses, it is 21.5%, which is significantly higher than the efficiency of a conventional thermoelement.

The structure of the CS in the MTE design has been substantiated, which consists of several contact layers that ensure the performance of the following functions: ohmic contact, adhesive, diffusion-barrier and commutation layers. Criteria for the selection of materials for the contact layers of the composite are substantiated. The factors determining the stability of the DBL are established and the materials for the DBL are determined. For deposition of contact layers, magnetron ion-plasma sputtering was used. The effective methods of surface preparation of samples of TE materials for the formation of CS were used. As a result of the analysis of the thermal stability of the CS using the Auger-electron method, the efficiency of the DBL was confirmed. Compounds with high adhesive strength (more than 14 MPa) and low contact resistance (about $10^{-9}\,\Omega \cdot m^2$) were obtained. To increase the thickness of the switching layer of Ni ($17-24\,\mu$m), its chemical deposition from borohydride electrolyte was used. The commutation of sections and tires in the MTE structure was carried out in several ways. Soldering was used at low temperatures. For commutation sections in MTE, at elevated temperatures, methods were used, implemented by: formation of Ni-In alloy; Ni-Sn eutectic alloy; using bonding of Au-Au layers.

As a result of the study of the temperature dependences of the TCLE of the materials, the following was established. The main problem area in the MTE structure at the contact of sections based on PbTe and GeTe with sections based on SiGe. In the temperature range of 900 K, the TCLE of the materials of these sections differ by a factor of 6. To eliminate mechanical stresses arising at high temperatures, it is proposed to form a damping layer of a composite material based on carbon nanotubes in the CS structure.

To assess thermal stability using differential scanning calorimetry, it was found that TE materials are thermally stable in the recommended ranges of operating temperatures. When using thermogravimetric analysis, it was determined that above a temperature of 850 K, intense sublimation begins for PbTe and GeTe. It has been experimentally established that protective layers of Si_3N_4 and SiO_2, obtained by plasma-chemical deposition eliminate sublimation of TE materials up to 1200 K.

Thus, in this work, ways are determined and methods for increasing the efficiency of generator thermoelements are justified. To implement these methods, a set of measures has been developed that determine the physical and technological foundations for the creation of multisection thermoelements, which make it possible to significantly increase the efficiency of TEG.

Funding

The reported study was funded by the grant of the President (Project No. 075-15-2020-441).

Conflict of interest

The authors declare that they have no conflict of interest.

References

[1] D. Zhao, G. Tan. Appl. Therm. Eng., **66**, 15 (2014).
[2] M. Shtern, M. Rogachev, Y. Shtern, A. Kozlov, A. Sherchenkov, E. Korchagin. In: Proc. 2021 International Seminar on Electron Devices Design and Production (Prague, Czech Republic, 2021) p. 9444502.
[3] A. Martinez, S. Diaz de Garayo, P. Aranguren, M. Araiz. Energy Convers. Manag., **2351**, 113992 (2021).
[4] Z. Soleimani, S. Zoras, B. Ceranic, S. Shahzad, Y. Cui. Energy Tech- nol. Assess, **37**, 100604 (2020).
[5] N. Jaziri, A. Boughamoura, J. Muller, B. Mezghani, F. Tounsi, M. Is- mail. Energy Rep., **6**, 264 (2020).
[6] Y. Ouyang, Z. Zhang, D. Li, J. Chen, G. Zhang. Annalen der Physik, **531** (4), 1800437 (2019).
[7] M. Shtern, M. Rogachev, Y. Shtern, A. Sherchenkov, A. Babich, E. Korchagin, D. Nikulin. J. Alloys Compd., **877**, 160328 (2021).
[8] A.A. Sherchenkov, Yu.I. Shtern, R.E. Mironov, M.Yu. Shtern, M.S. Rogachev. Nanotechnol. Russ., **10**, 827 (2015).
[9] E. Symeou, Ch. Nicolaou, A. Delimitis, J. Androulakis, Th. Kyratsi, J. Giapintzakis. J. Solid State Chem., **270**, 388 (2019).
[10] P. Dharmaiah, H.-S. Kim, C.-H. Lee, S.-J. Hong. J. Alloys Compd., **686**, 1 (2016).
[11] W.H. Shin, K. Ahn, M. Jeong, J.S. Yoon, J.M. Song, S. Lee, W.S. Seo, Y.S. Lim. J. Alloys Compd., **718**, 342 (2017).
[12] V. Ohorodniichuk, S. El-Oualid, A. Dauscher, C. Candolfi, P. Mass- chelein, S. Migot, P. Dalicieux, P. Baranek, B. Lenoir, J. Mater. Science, **55**, 1092 (2020).
[13] A.T. Burkov, S.V. Novikov, X. Tang, Y. Yan. Semiconductors, **51**, 1024 (2017).
[14] T. Zhu, Y. Liu, C. Fu, J.P. Heremans, J.G. Snyder, X. Zhao. Ad- vanced Mater., **29**, 1605884 (2017).
[15] A.A. Sherchenkov, Y.I. Shtern, M.Y. Shtern, M.S. Rogachev. Nano- technol. Russ., **11**, 287 (2016).
[16] G. Tan, L.-D. Zhao, M.G. Kanatzidis. Chem. Rev., **116**, 12123 (2016).
[17] M.Yu, Shtern, M.S. Rogachev, A.A. Sherchenkov, YuI. Shtern. Mater. Today: Proceedings, **84**, 295 (2020).
[18] S. Twaha, J. Zhu, Y. Yan, B. Li. Renew. Sustain. Energy Rev., **65**, 698 (2016).
[19] M.Yu. Shtern, I.S. Karavaev, Y.I. Shtern, A.O. Kozlov, M.S. Rogachev. Semiconductors. **53**, 1848 (2019).
[20] C.L. Cramer, H. Wang, K. Ma. J. Electron. Mater., **47**, 5122 (2018).
[21] P.H. Ngan, L. Han, D.V. Christensen. J. Electron. Mater., **47**, 701 (2018).
[22] L. Cai, P. Li, Q. Luo, P. Zhai, Q. Zhang. J. Electron. Mater., **46**, 1552 (2017).
[23] M. Shtern, M. Rogachev, Y. Shtern, D. Gromov, A. Kozlov, I. Kara- vaev. J. Alloys Compd., **852**, 156889 (2021).
[24] S.-W. Chen, A.H. Chu, D.S.-H. Wong. J. Alloys Compd., **699**, 448 (2017).
[25] H.-Y. Zhou, W.-Y. Zhao, G. Liu, H. Cheng, Q.-J. Zhang. J. Electron. Mater., **42**, 1436 (2013).
[26] X.Y. Yang, J.H. Wu, M. Gub, X.G. Xia, L.D. Chen. Ceram. Int., **42**, 8044 (2016).
[27] D.G. Gromov, Yu.I. Shtern, M.S. Rogachev, A.S. Shulyat'ev, E.P. Kirilenko, M.Yu. Shtern, V.A. Fedorov, M.S. Mikhailova, Inorg. Mater. **52**, 1132 (2016).

[28] J. de Boor, C. Gloanec, H. Kolb, R. Sottong, P. Ziolkowsk, E. Muller. J. Alloys Compd. **632**, 348 (2015).
[29] J. De Boor, D. Droste, C. Schneider, J. Janek, E. Mueller. J. Electron. Mater., **45**, 5313 (2016).
[30] T. Sakamoto, Y. Taguchi, T. Kutsuwa, K. Ichimi, S. Kasatani, M. In- ada. J. Electron. Mater., —bf45, 1321 (2016).
[31] S.H. Park, Y. Kim, C.Y. Yoo, G. Yoon. J. Vac. Sci. Technol. A, **34**, 061101 (2016).
[32] Y. Sadia, T. Ohaion-Raz, O. Ben-Yehuda, M. Korngold, Y. Gelbstein. J. Solid State Chem., **241**, 79 (2016).
[33] M.Yu. Shtern. In: Proceedings of the 2019 IEEE Conference of Rus- sian Young Researchers in Electrical and Electronic Engineering (Moscow, Russia, 2019), p. 1920.
[34] Yu. Stern, L. Pavlova, R. Mironov. J. Electron. Mater., **39** (9), 1422 (2010).
[35] Z.-G. Chen, G. Han, L. Yang, L. Cheng, J. Zou. Prog. Nat. Sci., **22**, 535 (2012).
[36] Thick and thin films for electronic applications, ed. by A. Reisman, K. Rose (N.Y., Wiley, 1971).
[37] S.M. Sze, K.K. Ng. Physics of Semiconductor Devices (N.Y., Wiley, 2007).
[38] E.H. Rhoderick, R.H. Williams. Metal-Semiconductor Contacts (Ox- ford, University Press, 1988).
[39] R. Yang, S. Chen, W. Fan, X. Gao, Y. Long, W. Wang, Z.A. Munir. J. Alloys Compd. **704**, 545 (2017).
[40] S.I. Novikova. Thermal expansion of solids (M., Nauka, 1974) [in Russian].
[41] S. Yoneda, M. Kato, I.J. Ohsugi. J. Appl. Phys., **107**, 074901 (2010).
[42] Y. Hikage, S. Masutani, T. Sato, S. Yoneda, Y. Ohno, Y. Isoda, Y. Imai, Y. Shinohara. In: Proceedings of the 26th International Conference on Thermoelectrics (Jeju, Korea, 2007) p. 331.
[43] H. Wiedemeir, P.A. Siemers. J. inor. and general chem., **431**, 299 (1977).
[44] A.S. Ohotin, A.A. Efremov, V.S. Ohotin, A.S. Pushkarskij. Thermoe- lectric generators (M., Atomizdat, 1971) [in Russian].
[45] V. Ravi, S. Firdosy, T. Caillat, E. Brandon, K. Van Der Walde, L. Maricic, A. Sayir. J. Electron. Mater., **38**, 1433 (2009).
[46] J.P. Dismukes, L. Ekstrom, R.J. Paff. J. Phys. Chem., **68**, 3021 (1964).
[47] V.M. Glazov, V.B. Kol'tsov, V.Z. Kutsova, A.R. Regel, Yu.N. Taran, G.G. Timoshina, E.S. Fal'kevich. Fizika i tekhnika poluprovodnikov, **25** (4), 588 (1991).
[48] Pat. No. 2601243 Method for producing thermoelectric element. Yu.I. Shtern, D.G. Gromov, M.S. Rogachev, M.Yu. Shtern, S.V. Dubkov [in Russian].